JOC*Note*

Highly Intense Fluorescent Diarylboron Diketonate

Atsushi Nagai, Kenta Kokado, Yuuya Nagata,
Manabu Arita, and Yoshiki Chujo*

*Department of Polymer Chemistry, Graduate School of
Engineering, Kyoto University, Katsura, Nishikyo-ku,
Kyoto 615-8510, Japan*

chujo@chujo.synchem.kyoto-u.ac.jp

Received August 8, 2008

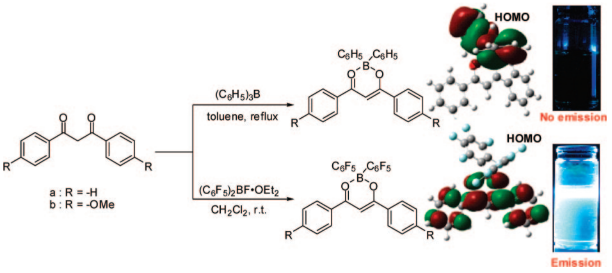

Diarylboron diketonates were successfully prepared by the reaction of 1,3-diketone derivatives and arylboron compounds such as triphenylborane [BPh_3] and fluorobis(pentafluorophenyl)borane diethyl etherate [$(C_6F_5)_2BF{\cdot}OEt_2$]. The fluorescent emission of their complexes took place depending on the substituent of the arylboron moiety. In particular, a boron 1,3-bis(4-methoxyphenyl)-1,3-diketonate chelated by a strong electron-withdrawing C_6F_5 group exhibited the most intense fluorescence.

The recent upsurge in the designing studies of fluorescent organoboron dyes such as 4,4-difluoro-4-bora-3a,4a-diaza-*s*-indacenes (BODIPYs) and boron diketonates reflects their features in the fields of molecular probes,[1] photosensitizers,[2] and lasers[3] because their dyes possess large molar extinction coefficients, two-photon absorption cross sections, high emission quantum yields, and sensitivity to the surrounding medium.[4] Boron diketonates are generally synthesized by treatment of bidentate organic π-chromophores with boron reagents such as trifluoroboron diethyl etherate ($BF_3{\cdot}OEt_2$), and are air-stable due to tetrahedral complexes with one chelating π-conjugated chromophore.[5] Recently, Fraser et al. have demonstrated that a hydroxy-functionalized difluoroboron dibenzoylmethane, which presented high fluorescence quantum yields (Φ_F) among reported boron diketonates, was prepared, and was employed as an initiator in the ring-opening polymerization of lactide to obtain BF_2-dibenzoylmethane end-functionalized polylactide. This compound also showed high Φ_F and room temperature phosphorescence.[6]

SCHEME 1. Synthesis of Diarylboron Diketonates

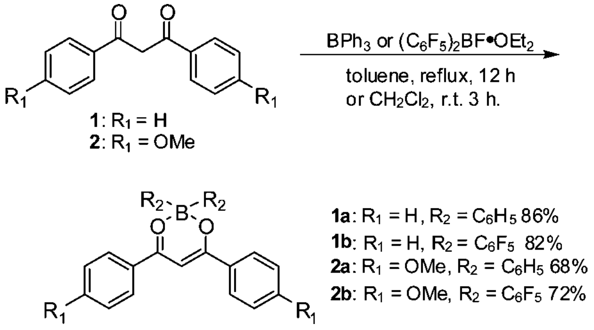

The presence of B−F bonds in the usual organoboron dyes results in some instability under irradiation and sensitivity to polar solvents. To date, to overcome these disadvantages, many BODIPY derivatives replacing fluoride with aryl, ethynylaryl, ethynylthienyl, and so on have been reported.[7] Such derivatives shared not only improvement of their stabilities but also large Stokes' shifts in their emission spectra, which is of paramount importance in multicolor labeling, i.e., chromosome mapping.[8] In contrast, only a diphenylboron diketonate as an analogous derivative has been recently reported,[9] and its luminescent property has not yet been investigated. This prompted us to expand the research of boron 1,3-diketonate dyes by designing emissive diarylboron complexes. In this paper, we report the synthesis, spectroscopic properties, and theoretical calculations of diarylboron diketonates.

Successive reaction between 1,3-diketone derivatives and boron reagents such as triphenylborane (BPh_3) and fluorobis(pentafluorophenyl)borane diethyletherate ($(C_6F_5)_2BF{\cdot}OEt_2$)[10] afforded the

---

(1) Haugland, R. P. *The Handbook—A Guide to Fluorescent Probes and Labeling Technologies*, 10th ed.; Spence, M. T. Z., Ed.; Molecular Probes: Eugene, OR, 2005; Chapter 1, Section 1.4.

(2) Gorman, A.; Killoran, J.; O'Shea, C.; Kenna, T.; Gallagher, W. M.; O'Shea, D. F. *J. Am. Chem. Soc.* **2004**, *126*, 10619.

(3) (a) García-Moreno, I.; Costela, A.; Campo, L.; Sastre, R.; Amat-Guerri, F.; Liras, M.; López Arbeloa, F.; Bañuelos Prieto, J.; López Arbeloa, I. *J. Phys. Chem. A* **2004**, *108*, 3315. (b) Pavlopoulos, T. G.; Boyer, J. H.; Sathyamoorthi, G. *Appl. Opt.* **1998**, *37*, 7797.

(4) Chow, Y. L.; Johansson, C. I.; Zhang, Y.-H.; Gautron, R.; Yang, L.; Rassat, A.; Yang, S.-Z. *J. Phys. Org. Chem.* **1996**, *9*, 7.

(5) (a) Maeda, H.; Mihashi, Y.; Haketa, Y. *Org. Lett.* **2008**, *10*, 3179. (b) Ono, K.; Yoshikawa, K.; Tsuji, Y.; Yamaguchi, H.; Uozumi, R.; Tomura, M.; Taga, K.; Saito, K. *Tetrahedron* **2007**, *63*, 9354. (c) Rohde, D.; Yan, C.-J.; Wan, L.-J. *Langmuir* **2006**, *22*, 4750. (d) Mirochnik, A. G.; Fedorenko, E. V.; Kuryavyi, V. G.; Bukvetskii, B. V.; Karasev, V. E. *J. Fluoresc.* **2006**, *16*, 279. (e) Cogné-Laage, E.; Allemand, J.-F.; Ruel, O.; Baudin, J.-B.; Croquette, V.; Blanchard-Desce, M.; Jullien, L. *Chem.—Eur. J.* **2004**, *10*, 1445. (f) Görlitz, G.; Hartmann, H.; Nuber, B.; Wolff, J. J. *J. Prakt. Chem.* **1999**, *341*, 167.

(6) Zhang, G.; Chen, J.; Payne, S. J.; Kooi, S. E.; Demas, J. N.; Fraser, C. L. *J. Am. Chem. Soc.* **2007**, *129*, 8942.

(7) (a) Bonardi, L.; Ulrich, G.; Ziessel, R. *Org. Lett.* **2008**, *10*, 2183. (b) Goeb, S.; Ziessel, R. *Org. Lett.* **2007**, *9*, 737. (c) Goze, C.; Ulrich, G.; Ziessel, R. *J. Org. Chem.* **2007**, *72*, 313. (d) Goze, C.; Ulrich, G.; Ziessel, R. *Org. Lett.* **2006**, *8*, 4445. (e) Goze, C.; Ulrich, G.; Mallon, L. J.; Allen, B. D.; Harriman, A.; Ziessel, R. *J. Am. Chem. Soc.* **2006**, *128*, 10231. (f) Ulrich, G.; Goze, C.; Goeb, S.; Retailleau, P.; Ziessel, R. *New J. Chem.* **2006**, *30*, 982.

(8) Ju., J.; Ruan, C.; Fuller, C. W.; Glazer, A. N.; Mathies, R. A. *Proc. Natl. Acad. Sci. U.S.A.* **1995**, *92*, 4347.

(9) Bally, I.; Arsene, A.; Bacesou-Roman, M.; Balaban, A. T. *Tetrahedron Lett.* **1965**, 3929.

(10) (a) Yoshio, J.; Kano, N.; Kawashima, T. *Chem. Commun.* **2007**, 559. (b) Duchateau, R.; Lancaster, S. J.; Thornton-Pett, M.; Bochamnn, M. *Organometallics* **1997**, *16*, 4995.

10.1021/jo8017582 CCC: $40.75

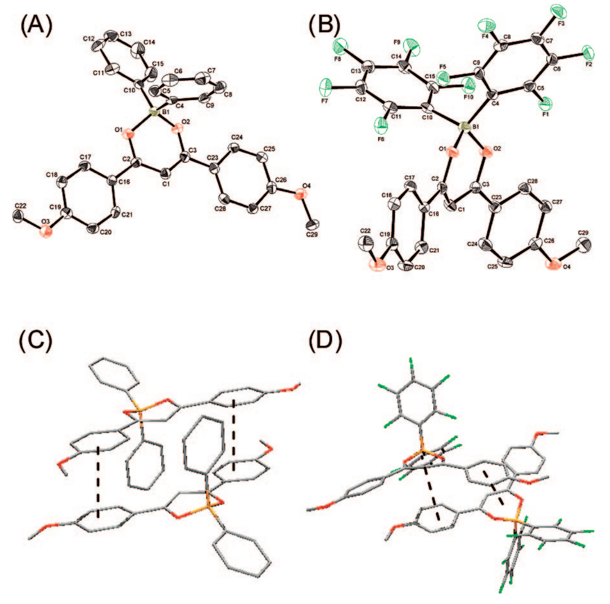

FIGURE 1. ORTEP drawings of **2a** (A) and **2b** (B). Thermal ellipsoids are drawn at the 50% propability level. Crystal packing structures of **2a** (C) and **2b** (D).

corresponding boron diketonates **1a**, **1b**, **2a**, and **2b** in good yields, respectively (Scheme 1). The tetracoordination states of the boron atoms of **1a**−**2b** were confirmed by the ^{11}B NMR spectroscopy in CDCl$_3$. The spectra of **1a** ($\delta_B = 8.79$ ppm) and **1b** ($\delta_B = 8.11$ ppm) were downfield-shifted toward those of **2a** ($\delta_B = 5.47$ ppm) and **2b** ($\delta_B = 5.08$ ppm), probably resulting in the substitution for each 1,3-diketone ligand (discussed later). Further, the basic structures of the obtained diketonates were also characterized by ^{1}H and ^{13}C NMR, IR and electron ionization mass spectroscopies, and elemental analysis.

The crystallographically determined molecular structures of **2a** and **2b** are shown in Figure 1A,B.[11] The sp^3 orbits hydridized at boron centers of **2a** and **2b** appear as a distorted tetrahedron with bond angles O2−B1−O1 of 107.3° and 108.6°, respectively, slightly narrower than what is observed in difluoroboron diketonate (111.7°),[5b] and the angles of C4−B1−C10 were 115.1° and 110.7°, respectively. The average B−O bond length of **2a** (1.52 Å) was slightly longer than that of **2b** (1.49 Å), whose value is comparable to those found in difluoroboron diketonate analogues (1.48 Å), and the average of bond length betweenthe boron atom and the aromatic carbon atom (B−C4 and B−C10) of **2a** (1.61 Å) was slightly shorter than that of **2b** (1.63 Å). These data indicate that the electron density of a boron atom in **2b** is poorer than that of **2a** due to the strong electron-withdrawing C$_6$F$_5$ group, i.e., the chelating ability of **2b** is higher than that of **2a**. Panels C and D of Figure 1 illustrate the crystal packing structures of **2a** and **2b**. The intermolecular distance of **2a** is 3.68 Å, indicating effective $\pi-\pi$ stacking between neighboring phenyl groups. Further, the packing structure of **2b** is interacted between distort boron chelating and phenyl rings at a length of 3.17 Å (Figure 1C,D). These results could indicate that the structures of **2a** and **2b** take the tetrahedral structures on each boron center.

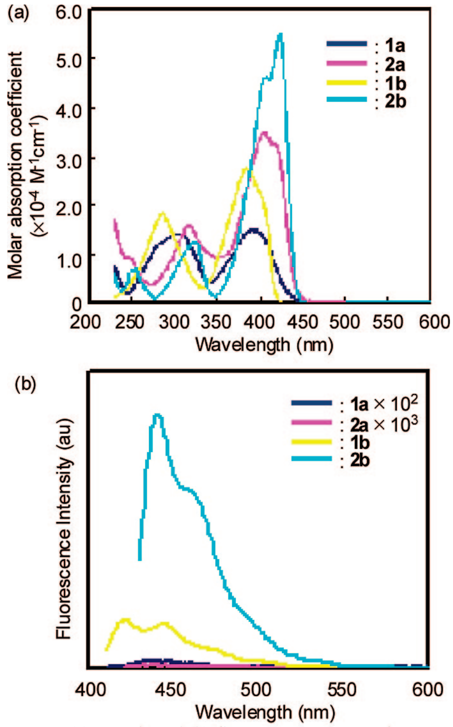

FIGURE 2. (a) UV−vis and (b) fluorescence spectra of **1a**, **1b**, **2a**, and **2b** in CH$_2$Cl$_2$ (1.0 × 10^{-5} mol/L).

To examine the optical properties of the obtained boron diketonates, UV−vis absorption and photoluminescence experiments were carried out in CH$_2$Cl$_2$. The absorption maxima of **2** (**2a**: $\lambda_{max} = 405$ nm; and **2b**: $\lambda_{max} = 425$ nm) are red-shifted as compared to those of **1** (**1a**: $\lambda_{max} = 393$ nm; and **1b**: $\lambda_{max} = 385$ nm), and the molar absorption coefficients of **2** (**2a**: $\epsilon = 3.5 \times 10^4$ M^{-1} cm^{-1}; and **2b**: $\epsilon = 5.5 \times 10^4$ M^{-1} cm^{-1}) are also higher than those of **1** (**1a**: $\epsilon = 1.5 \times 10^4$ M^{-1} cm^{-1}; and **1b**: $\epsilon = 2.7 \times 10^4$ M^{-1} cm^{-1}) (Figure 2A), corresponding to $\pi \rightarrow \pi^*$ transition.[12] These results suggest that the changes of these shifted absorptions and coefficients reflect in the electronic structures of ligand moieties, irrespective of those on boron atoms. In the fluorescence spectra in CH$_2$Cl$_2$, **1b** and **2b** showed emission maxima at 421 (excited at 385 nm) and 441 nm (excited at 425 nm), respectively (Figure 2A). The absolute fluorescence quantum yields of **1b** and **2b** in CH$_2$Cl$_2$ at room temperature were determined as $\Phi_F = 0.27$ and 0.86, respectively, which are high enough Φ_F as compared with those of any BF$_2$ chelating diketone derivatives reported previously.[5,6] In contrast, **1a** and **2a** showed almost no fluorescent emission (**1a**: $\Phi_F \leq 0.01$; and **2a**: $\Phi_F = 0.06$). The substituents on the boron atoms should be responsible for the intensity of fluorescence, considering the above results.

To investigate the redox properties of the diarylboron diketonates, cyclic voltammetry (CV) in acetonitrile was performed (see the Supporting Information, Figure 1S). The voltammograms showed reversible waves for them. No clear oxidation waves were observed up to + 2.0 V versus Ag/Ag$^+$. The reduction potential (E) of **1a** ($E = -1.40$ V) was lower than that of **2a** ($E = -1.57$ V), indicating that the electron affinity of **1a** increases as compared to that of **2a**, i.e., the

---

(11) (a) The crystal data for **2a** are as follows. C$_{29}$H$_{25}$BO$_4$, FW = 448.30, triclinic, $P\bar{1}$, $a = 8.36$ (3) Å, $b = 13.64$ (6) Å, $c = 20.85$ (10) Å, $\alpha = 101.61(15)°$, $\beta = 95.4(2)°$, $\gamma = 94.3(2)°$, $V = 2307$ (17) Å^3, $Z = 4$, $D_{calcd} = 1.291$ g cm^{-3}; the refinement converged to $R = 0.059$, $R_w = 0.139$, GOF = 0.851. (b) The crystal data for **2b** are as follows. C$_{29}$H$_{15}$BF$_{10}$O$_4$, FW = 628.22, monoclinic, $P\bar{2}1/c$, $a = 19.8126$ (18) Å, $b = 10.6735$ (10) Å, $c = 25.2963$ (17) Å, $\alpha = 90°$, $\beta = 106.387(4)°$, $\gamma = 90°$, $V = 5132.1$ (8) Å^3, $Z = 8$, $D_{calcd} = 1.626$ g cm^{-3}; the refinement converged to $R = 0.050$, $R_w = 0.075$, GOF = 0.956.

(12) (a) Ilge, H.-D.; Birckner, E.; Fassler, D.; Kozmenko, M. V.; Kuz'min, M. G.; Hartmann, H. *J. Photochem.* **1986**, *32*, 177. (b) Morgan, G. T.; Tunstall, R. B. *J. Chem. Soc.* **1924**, *125*, 1963.

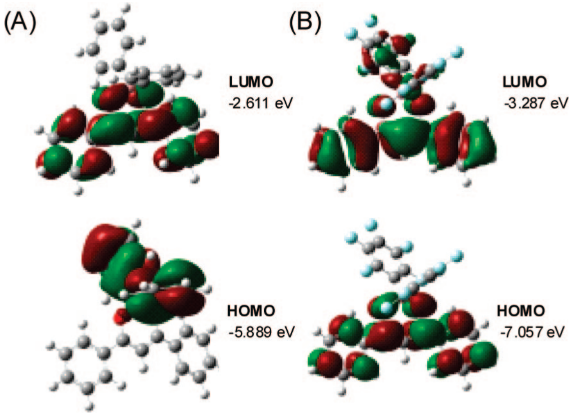

FIGURE 3. Molecular orbital diagrams for the LUMO and HOMO of **1a** (A) and **1b** (B) (B3LYP/6-31G(d, p)//B3LYP/6-31G(d, p)).

electron density around the boron atom of **2a** having methoxy groups is higher than that of **1a**. The relationship of **1b** ($E = -1.18$ V) and **2b** ($E = -1.30$ V) was the same. From these results, the ^{11}B NMR chemical shifts of **1a**−**2b** indicate that substitution of methoxy groups for the 1,3-diketone ligand strongly influences the chelating moiety as compared to that of aryl groups.

To provide a more effective understanding for the emission behavior of **1a**−**2b**, we employed the theoretical calculation using the density-functional theory (DFT) method at the B3LYP/6-31G(d p)//B3LYP/6-31G(d,p). Parts A and B of Figure 3 exhibit the lowest unoccupied molecualr orbital (LUMO) and the highest occupied molecular orbital (HOMO) of **1a** and **1b**, respectively. The π orbital of the 1,3-diketone group of **1b** lies on their LUMO and HOMO. As a result, the $\pi \rightarrow \pi^*$ excited state of **1b** occupies the lowest excited state, and the transition between the excited state and ground state is allowed. In contrast, the HOMO of **1a** is not on the 1,3-diketone moieties but localized on the whole of the phenyl groups. The relatively high energy level of the occupied orbitals of phenyl groups prevents the HOMO from locating the π orbital on 1,3-diketone group of **1a**, i.e., the fluorescence quantum yield is extremely low, analogizing with the emissive driving force of boron-substituted azobenzenes reported previously by Kawashima et al.[10a] The DFTs of **2a** and **2b** were also identical (see the Supporting Information, Figure 2S). Therefore, the emission behavior of diarylboron diketonates should originate from HOMO inverted by the strong electron-withdrawing C_6F_5 groups.

In conclusion, we have described the synthesis of highly intense fluorescent diarylboron diketonates, and illustrated the emission behavior of diarylboron diketonates by UV−vis and photoluminescence spectroscopies, and theoretical calculation using density-functional theory (DFT). To the best of our knowledge, this is the first example of the designs of diarylboron diketonates with fluorescence. We are currently extending this procedure to the design and synthesis of higher intense fluorescent diarylboron diketonates applicable to fluorescent probes of chemical sensors and organic electroluminescent devices.

Experimental Section

Synthesis of 1a. BPh_3 (1.21 g, 5.00 mmol) was added to a solution of 1,3-diphenyl-1,3-propanedione (0.22 g, 1.00 mmol) in dry toluene (4.0 mL) under nitrogen atmosphere. After the reaction mixture was refluxed at 120 °C for 12 h, the solvent was removed in vacuo. The residual product was purified by silica gel column chromatography eluted with *n*-hexane/$CHCl_3$ [2:1(v/v)], followed by recrystallization from dichloromethane/*n*-hexane to obtain **1a** (0.34 g, 0.87 mmol) in 87% yield as a yellowish powder. ^1H NMR ($CDCl_3$) δ 6.99 (s, 1H, $-CH{=}C{<}$), 7.20−7.29 (m, 6H, aromatic protons), 7.52−7.68 (m, 10H, aromatic protons), 8.18 (d, $J = 7.3$ Hz, 4H, aromatic protons) ppm. ^{13}C NMR ($CDCl_3$) δ 182.9, 134.3, 133.2, 131.3, 129.0, 128.5, 127.2, 126.5, 94.1 ppm. ^{11}B NMR ($CDCl_3$) δ 8.79 ppm. IR (NaCl) ν 1540, 1522, 1490, 1355, 1205, 706 cm^{-1}. HRMS (EI) calcd for $C_{27}H_{21}O_2B$ (M^+) *m*/*z* 388.1635, found *m*/*z* 388.1635. Anal. Calcd for $C_{27}H_{21}O_2B$: C, 83.52; H, 5.45. Found: C, 83.32; H, 5.41.

Synthesis of 1b. $(C_6H_5)_2BF{\cdot}OEt_2$ (1.71 g, 3.90 mmol) was added to a solution of 1,3-diphenyl-1,3-propanedione (0.18 g, 0.78 mmol) in dry dichloromethane (6.0 mL) under nitrogen atmosphere. The reaction mixture was stirred at room temperature for 3.0 h. After the insoluble materials were removed by filtration, the solvent was evaporated in vacuo. The residual product was purified by silica gel column chromatography eluted with *n*-hexane/$CHCl_3$ [4:1(v/v)], followed by recrystallization from dichloromethane/*n*-hexane to obtain **1b** (0.36 g, 0.63 mmol) in 82% yield as a yellowish powder.^1H NMR ($CDCl_3$) δ 7.16 (s, 1H, $-CH{=}C{<}$), 7.56 (t, $J =$ 7.8 and 15.6 Hz, 3H, aromatic protons), 7.73 (t, $J = 7.3$ and 14.6 Hz, 3H, aromatic protons), 8.19 (d, $J = 7.6$ Hz, 4H, aromatic protons) ppm. ^{13}C NMR ($CDCl_3$) δ 180.0, 164.5, 131.3, 130.7, 127.1, 126.3, 125.9, 114.3, 92.1, 55.6 ppm. ^{11}B NMR ($CDCl_3$) δ 5.47 ppm. IR (NaCl) ν 3082, 1539, 1533, 1489, 1475, 1349, 1105, 974, 717 cm^{-1}. HRMS (EI) calcd for $C_{27}H_{11}O_2F_{10}B$ (M^+) *m*/*z* 568.0688, found *m*/*z* 568.0692. Anal. Calcd for $C_{27}H_{11}O_2F_{10}B$: C, 57.08; H, 1.95. Found: C, 57.33; H, 2.21.

Synthesis of 2a. Similarly to the preparation of **1a**, **2a** was prepared from 1,3-bis(4-methoxyphenyl)-1,3-propanedione (0.22 g, 0.78 mmol) and BPh_3 (0.95 g, 3.91 mmol) in dry toluene (4.0 mL) in 68% (0.24 g, 0.53 mmol) yield as a yellow crystal. ^1H NMR ($CDCl_3$) δ 3.90 (s, 6H, $-OCH_3 \times 2$), 6.82 (s, 1H, $-CH{=}C{<}$), 7.00 (d, $J = 9.0$ Hz, 4H, aromatic protons), 7.18−7.28 (m, 6H, aromatic protons), 7.61 (d, $J =$ 6.8 Hz, 4H, aromatic protons), 8.14 (d, $J = 8.8$ Hz, 4H, aromatic protons) ppm. ^{13}C NMR ($CDCl_3$) δ 183.1, 149.4, 147.0, 141.6, 139.2, 138.4, 135.9, 135.5, 132.0, 131.9, 129.3. 129.2, 129.2, 93.8 ppm. ^{11}B NMR ($CDCl_3$) δ 8.11 ppm. IR (NaCl) ν 3045, 1605, 1542, 1493, 1242, 1174, 784 cm^{-1}. HRMS (EI) calcd for $C_{29}H_{25}O_4B$ (M^+) *m*/*z* 448.1846, found *m*/*z* 448.1841. Anal. Calcd for $C_{29}H_{25}O_4B$: C, 77.69; H, 5.62. Found: C, 77.42; H, 5.65.

Synthesis of 2b. Similarly to the preparation of **1b**, **2b** was prepared from 1,3-bis(4-methoxyphenyl)-1,3-propandione (0.22 g, 0.78 mmol) and $(C_6H_5)_2BF{\cdot}OEt_2$ (1.71 g, 3.90 mmol) in dry dichloromethane (6.0 mL) in 72% (0.35 g, 0.56 mmol) yield as a yellow crystal. ^1H NMR ($CDCl_3$) δ 3.93 (s, 6H, $-OCH_3 \times 2$), 6.95 (s, 1H, $-CH{=}C{<}$), 7.04 (d, $J = 9.0$ Hz, 4H, aromatic protons), 8.15 (d, $J = 8.8$ Hz, 4H, aromatic protons) ppm. ^{13}C NMR ($CDCl_3$) δ 180.5, 165.5, 149.4, 146.8, 141.6, 139.01, 138.1, 135.8, 131.5, 124.5, 114.6, 92.0, 55.7 ppm. ^{11}B NMR ($CDCl_3$) δ 5.08 ppm. IR (NaCl) ν 1604, 1558, 1541, 1506, 1495, 1240, 1173, 1097, 978 cm^{-1}. HRMS (EI) calcd for $C_{29}H_{15}O_4F_{10}B$ (M^+) *m*/*z* 628.0904, found *m*/*z* 628.0903. Anal. Calcd for $C_{29}H_{15}O_4F_{10}B$: C, 55.44; H, 2.41. Found: C, 55.65; H, 2.43.

Acknowledgment. We thank Dr. Y, Morisaki and Dr. K, Tanaka for helpful discussions at Kyoto University.

Supporting Information Available: Text giving typical experimental procedures, copies of NMR spectra, Figure 1S showing CVs of **1a**−**2b**, Figure 2S showing the LUMO and HOMO of **2a** and **2b**, and crystal structural data for **2a** and **2b**. This material is available free of charge via the Internet at http://pubs.acs.org.

JO8017582